 CMC, vol.31, no.2, pp.127-146, 2012

On the Compression Viewed as a Geometric Transformation

Ligia Munteanu[1], **Cornel Brisan**[2], **Veturia Chiroiu**[3]
Stefania Donescu [4]

Abstract: A modeling of the compression by using the property of Helmholtz equation to be invariant under geometric transformations is presented in this paper. The versatility of the geometric transformations is illustrated in order to obtain a new interpretation of the compression process. The physical spatial compression leads, most of the times, to new materials with inhomogeneous and anisotropic properties. The compression can be theoretically controlled by the geometric transformations. As an example, new architectures for auxetic materials can be built up by applying the geometric transformations. The new versions are finding their full correspondents in the results of the experiments in which the conventional foams are subjected to compressive cyclic loading.

Keywords: Compression, Geometric transformation, Auxetic foams, Cosserat theory.

1 Introduction

Pendry, Shurig and Smith (2006) proved that a finite size object surrounded by a coating consisting of a specially designed metamaterial would become invisible for electromagnetic waves at any frequency. The idea is that the sound sees the space differently [Dupont *et al*. (2011)]. For the sound, the concept of distance is modified by the acoustic properties of the regions through which the sound travels. In geometrical acoustics, the idea of the acoustical path when travelling an infinitesimal distance ds, is the corresponding acoustical path length $c^{-1}\mathrm{d}s$, where $c^{-1}=\sqrt{\rho/\kappa}$

[1] Institute of Solid Mechanics of Romanian Academy, Dept. of Deformable Media and Ultrasonics, Bucharest
[2] Technical University of Cluj-Napoca, Dept. of Mechatronics and System Dynamics, Cluj-Napoca
[3] Institute of Solid Mechanics of Romanian Academy, Dept. of Deformable Media and Ultrasonics, Bucharest
[4] Technical University of Civil Engineering, Bucharest, Dept. of Mathematics and Computer Science, Bucharest

with ρ is the fluid density and κ is the compression modulus of the fluid. Cummer and Schurig (2007) demonstrated that acoustic waves in a fluid undergo the same geometric transformation as electromagnetic waves do and therefore retain their form. For example, the 3D equation for the pressure waves propagating in a bounded fluid region $\Omega \subset \mathrm{R}^3$ is the Helmholtz equation

$$\nabla \cdot (\rho^{-1} \nabla p) + \frac{\omega^2}{\kappa} p = 0, \tag{1.1}$$

where p is the pressure, ρ is the rank-2 tensor of the fluid density, κ is the compression modulus of the fluid, and ω is the wave frequency.

Geometric transformations applied to certain types of elastodynamic waves in structural mechanics received less attention, since the Navier equations do not usually retain their form under geometric changes [Bigoni *et al.* (1998); Norris (2008)]. For example, the in-plane propagation of time-harmonic elastic waves is governed by the Navier equations

$$\nabla \cdot C : \nabla U + \rho \omega^2 U + b = 0, \tag{1.2}$$

where u is the displacement, ρ the density, C the 4th-order material tensor of the linear elastic material and $b(x)$ represents the spatial distribution of a simple harmonic body force $\hat{b}(x,t) = b(x)\exp(\mathrm{i}\omega t)$, with the wave-frequency and t the time. Brun, Guenneau and Movchan (2009) demonstrated that the Navier equations (1.2) retain their form under the transformation

$$r' = r_0 + \frac{r - r_{01}}{r_1} r, \quad \theta' = \theta \tag{1.3}$$

for $r \leq r_1$, $r = r'$, $\theta = \theta'$, for $r > r_1$, where r_0 and r_1 are the inner and outer radii of the circular domain, respectively.

Let us consider the geometric transformation from the coordinate system (x', y', z') of the compressed space to the original coordinate system(x, y, z), given by$x(x', y', z')$, $y(x', y', z')$ and $z(x', y', z')$. The change of coordinates is characterized by the transformation of the differentials through the Jacobian J of this transformation, i.e.

$$\begin{pmatrix} \mathrm{d}x \\ \mathrm{d}y \\ \mathrm{d}z \end{pmatrix} = J_{xx'} \begin{pmatrix} \mathrm{d}x' \\ \mathrm{d}y' \\ \mathrm{d}z' \end{pmatrix}, \tag{1.4}$$

From the geometrical point of view, the change of coordinates implies that, in the transformed region, one can work with an associated metric tensor [Zolla *et al.* (2007); Guenneau *et al.* (2011)]

$$T = \frac{J_{xx'}^{\mathrm{T}} J_{xx'}}{\det(J_{xx'})}. \tag{1.5}$$

In terms of the material parameters, one can replace the material from the original domain (homogeneous and isotropic) by an equivalent compressed one that is inhomogeneous (its characteristics depend on the spherical (r', θ', ϕ') coordinates) and anisotropic (described by a tensor), and whose properties, in terms of $J_{x'x}$, are given by

$$\rho' = J_{x'x}^{-\mathrm{T}} \cdot \rho \cdot J_{x'x}^{-1} \cdot \det(J_{x'x}), \quad \kappa' = \kappa \det(J_{x'x}), \tag{1.6}$$

or, equivalently, in terms of $J_{xx'}$

$$\rho' = \frac{J_{xx'}^{\mathrm{T}} \cdot \rho \cdot J_{x'x}}{\det(J_{xx'})}, \quad \kappa' = \frac{\kappa}{\det(J_{xx'})}. \tag{1.7}$$

Here, ρ' is a second order tensor. When the Jacobian matrix is diagonal, (1.6) and (1.7) can be more easily written. Multiplying (1.1) by a test function φ and integrating by parts, one obtains [Dupont *et al*. (2011)]

$$-\int_{\Omega} \left(\nabla_{(x,y,z)}\varphi \cdot \rho^{-1} \nabla_{(x,y,z)} p\right) \mathrm{d}V + \int \left(\omega^2 \kappa^{-1} p\varphi\right) \mathrm{d}V = 0. \tag{1.8}$$

In (1.8) the surface integral, corresponding to a Neumann integral over the boundary $\partial\Omega$, is zero. By applying the coordinate transformation $(x, y, z) \to (x', y', z')$ to (1.8) and using (1.4), one obtains

$$-\int_{\Omega} \left(J_{x'x}^{\mathrm{T}} \nabla_{(x',y',z')}\varphi \cdot \rho^{-1} J_{x'x}^{\mathrm{T}} \nabla_{(x,y,z)} p\right) \det(J_{xx'}) \mathrm{d}V' + \int \left(\det(J_{xx'}) \omega^2 \kappa^{-1} p\varphi\right) \mathrm{d}V' = 0, \tag{1.9}$$

in terms of $J_{xx'}$, and

$$-\int_{\Omega} \left(\left(\nabla_{(x',y',z')}\varphi\right)^{\mathrm{T}} \frac{J_{x'x} \rho^{-1} J_{x'x}^{\mathrm{T}}}{\det(J_{x'x})} \nabla_{(x',y',z')} p \right) \mathrm{d}V' + \int \left(\frac{\kappa^{-1}}{\det(J_{x'x})} \omega^2 p\varphi \right) \mathrm{d}V' = 0, \tag{1.10}$$

in terms of $J_{x'x}$.

This theory is applied in this paper to model the compression of the conventional foams. The scope is to transform conventional foam which occupies the disk $r \leq R_2$ into auxetic material which fills the annulus$R_1 \leq r \leq R_2$. The new material is inhomogeneous and anisotropic. The problem is related to the current research in invisibility cloaks starting from the works by Pendry, Schurig and Smith (2006) ; Brun,

Guenneau and Movchan (2009) (cloaking via changes of coordinates); Leonhardt (2006) (cloaking via conformal mapping); Milton and Nicorovici (2006) (cloaking by reaction); Alu and Engheta (2003, 2005) (plasmonic cloaking); Greenleaf, Lassas and Uhlmann (2003) (cloaking in inverse problems); Milton (2007) (elastic metamaterials); Munteanu and Chiroiu (2011) (acoustic cloaking); Cummers *et al*. (2008) (seismic cloaking); Fu, Chen and Qin (2011); Marin and Karageorghis (2009); Johansson and Marin (2009): (variational aspects); Kalidindi *et al*. (2010) (building material knowledge systems).

Milton, Briane and Willis (2006) showed that geometric transformations cannot be applied to equations which are not invariant under coordinate transformations and, consequently, if cloaking exists for such equations (for example the elasticity equations), it would be of a different nature from acoustic and electromagnetic.

The touchstone of our technique is that the governing equations of the non-auxetic foams are invariant under geometric transformations, more precisely, the equations are reduced to the Helmholtz equations.

2 Formulation of the Problem

The geometric transformation may be linear or nonlinear. A linear geometric transformation (1.4) which maps the disk $r \leq R_2$ into an annulus $R_1 \leq r \leq R_2$ [Pendry, Schurig and Smith (2006); Chen and Lakes (1989)] is given by

$$r' = R_1 + r\frac{R_2 - R_1}{R_2}, \quad 0 \leq r \leq R_2,$$

$$\theta' = \theta, \quad 0 \leq \theta \leq 2\pi, \tag{2.1}$$

$$x_3' = x_3, \quad x_3 \in \mathrm{R},$$

where r', θ', x_3' are radially contracted cylindrical coordinates r, θ, x_3. The Cartesian basis (x_1, x_2, x_3) is defined as $x_1 = r\cos\theta$, $x_2 = r\sin\theta$. The Jacobean of the transformation from polar to stretched polar coordinates is given by J. In the stretched space, the associated metric tensor is given by (1.5)

$$T = \frac{J_{rr'}^{\mathrm{T}} J_{rr'}}{\det(J_{rr'})}. \tag{2.2}$$

Qiu *et al.* (2009) classified the geometric transformation functions in terms of the negative (i.e., concave-down) or positive (i.e., concave-up) sign of the second order derivative of this function. The concave-down nonlinear transformation compresses

a sphere of radius R_2 in the original space Ω into a shell region $R_1 < r' < R_2$ in the compressed space Ω' as

$$r(\beta) = \frac{R_2^{\beta+1}}{R_2^{\beta} - R_1^{\beta}} \left(1 - \left(\frac{R_1}{r'} \right)^{\beta} \right), \tag{2.3}$$

where β denotes the degree of the nonlinearity in the transformation. By taking $\beta \to 0$ in (2.3), the linear case is obtained, namely

$$r(\beta) = \frac{R_2 \mathrm{Ln}(r'/R_1)}{\mathrm{Ln}(R_2/R_1)}. \tag{2.4}$$

All curves belonging to (2.3) have negative second order derivative with respect to the physical space r'. This class of transformations is termed as the *concave-down* transformation. The transformation function (2.3) depends on the radial component r' in the spherical coordinate system (r', θ', ϕ').

The concave-up nonlinear transformation compresses a sphere of the radius R_2 in the original space Ω into a shell region $R_1 < r' < R_2$ in the compressed space Ω' as

$$r(\beta) = \frac{R_2 R_1^{\beta}}{R_2^{\beta} - R_1^{\beta}} \left(\left(\frac{r'}{R_1} \right)^{\beta} - 1 \right). \tag{2.5}$$

As $\beta \to 0$, one obtains again the linear case (2.4). This class of transformations is termed as the *concave-up* transformation because (2.5) has positive second order derivatives.

Once the above geometric transforms are written, let us formulate the problem to be solved in this paper. Let us suppose that the original domain is a cylinder of radius R_2 and length l. This domain is filled with conventional non-auxetic cellular foam. The spatial compression is obtained by applying the geometric transformation (2.1). The transformed domain is a shell cylinder of internal and external radii R_1 and R_2, respectively, and the length l'.

As example, this paper is building new architectures for auxetic materials by applying the geometric transformations. These theoretically versions find their full correspondents in the experiments of compression the conventional foams.

In the following we present the basic elements regarding the auxetic materials. The term *auxetic* is coming from the Greek word *auxetos*, meaning *that which may be increased*. Instead of getting thinner like an elongated elastic band, the auxetic material grows fatter, expanding laterally when stretched [Lakes (1986), (1987), (1991)]. Since 1987, when isotropic auxetic foam was manufactured for the first

time, negative Poisson's ratio materials have created interest for potential engineering applications. A feature that the auxetic materials showed compared to the other foams is the significant damping capacity with increase up to 16 times compared to the conventional foam [Scarpa *et al.* (2006); Chiroiu *et al.* (2009); Evans (1991); Donescu, Chiroiu and Munteanu (2009)]. Scientists have known about auxetic materials for over a hundred years, though without giving them much a special attention, and treating them as an accident or a curiosity [Alderson, Alderson and Evans (1997)]. The auxetic behavior is found in materials from the molecular and microscopic levels, up to the macroscopic level. Negative Poisson's ratios are observed in real materials with a high degree of anisotropy, such as honeycomb structures, reticulated metal foams, re-entrant structures, the skin covering a cow's teats, certain rocks and minerals, living bone tissue, etc. All the major classes of polymers, composites, metals and ceramics, can exist in the auxetic version [Mihailescu and Chiroiu (2005)].

Cellular solids are two phase composite materials in which one phase is a solid and the other is a fluid, most often air. The positive Poisson's ratio is the result of the convex shape of cell surfaces. By volume compression, a part of the cell surface may acquire first a zeroth and then negative curvature. When the number of such inverted cells dominates, compressibility of the material rises till the appearance of the negative Poisson's ratio [Shilko and Konyok (2004); Gaspar *et al.* (2005)].

Figure 2.1 shows the simplest 2D lattice structures for closed-cell solids: (a) square structure, (b) rectangle structure, (c) regular hexagonal structure, d) triangular structure and d) irregular structure. Figure 2.2 illustrates models of auxetic structures obtained from aforementioned materials by appearance of the negative Poisson's ratio: a), b) re-entrant honeycomb network, c) Shilko and Konyok model of the inverted closed-cell foam, and d) re-entrant regular array of rectangular nodules interconnected by fibrils [Evans and Alderson (2000)].

The conventional foam exhibits pores with average diameter around 1mm while the auxetic foam has average diameter possible down to a few micrometers or down to a few nanometers.

A comparative analysis between the cyclic loading compressive behaviour of conventional non-auxetic foam and the auxetic foams was performed by Bezazi and Scarpa in 2007. They analyzed the transformation of conventional foam into its auxetic version using a manufacturing process involving compression [Chan and Evans (1997); Scarpa *et al.* (2004)].

Bezazi and Scarpa (2007) used cylindrical foam samples of 30 mm of diameter and 170 mm of length, and after compression they obtained final diameter of 20 mm and length of 100 mm. The measured density of the auxetic foam was 0.118g / cm^3.

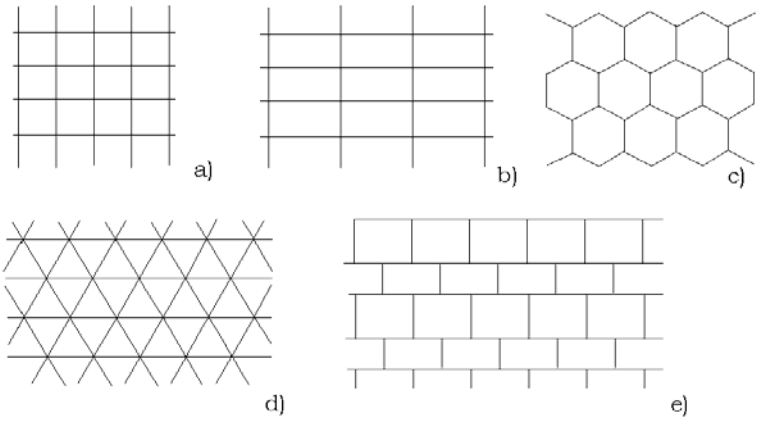

Figure 2.1: Regular 2D cellular solids.

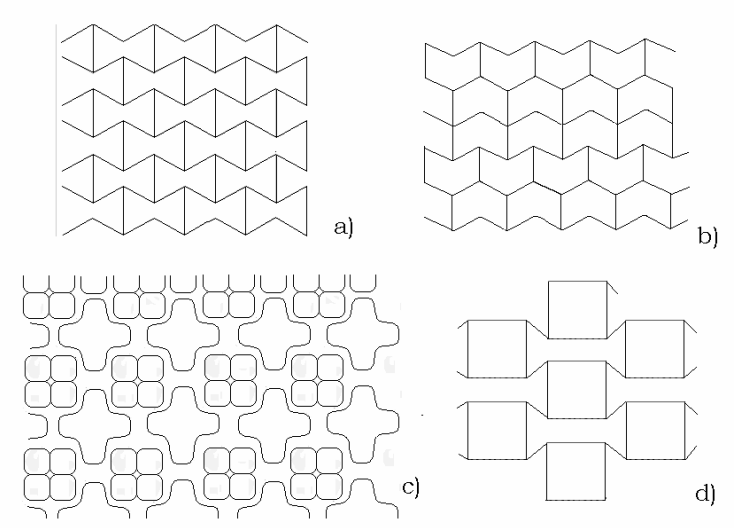

Figure 2.2: Model structures of the inverted closed-cell foam.

The Poisson's ratio depends on the compressive strain. So, the conventional foam has a Poisson's ratio positive of 0.25 at compressive strain of 10%, which decreases sharply with the increase of compressive loading, to become slightly negative from 60 to 80% of tensile strain. The auxetic foam exhibits a negative Poisson's ratio of -0.185 at compressive strain from 10 to 25%, showing a sharp increase for rising compressive strain, reaching then a zero value at 55% of compressive strain and a positive Poisson's ratio of 1.33 at 80%. The results of the compressive Poisson's ratio of auxetic foams obtained by Bezazi and Scarpa in 2007, are consistent with the ones presented in the literature [Scarpa *et al.* (2004); Blake and Isard (1998); Scarpa, Ciffo and Yates (2004); Lakes and Elms (1993)].

3 The Theory of Auxetic Materials

In order to write the equations governing the behavior of the conventional non-auxetic cellular foam, we remind that the microstructure of these foams can be modeled by the micropolar theory.

For this, we suppose that the material is a micropolar solid with chiral effects, i.e. a noncentrosymmetric material. The micropolar and classical theories of elasticity are continuum theories, which make no reference to atoms or other structural features of the material, which is described. Elasticity theory represents more than an analytical description of the phenomenological behavior since it can be derived as a first approximation of the interaction between atoms in the solid [Cosserat (1909); Kröner (1963)]. Interatomic forces are of short range; but they exert more influence than one atomic space. The characteristic length l in this case should be on the order of the atomic spacing. Phenomena associated with micropolar elasticity are likely to be of larger magnitude, and therefore of greater interest in materials such as cellular solids with larger scale structural features. In fibrous composites, the characteristic length l may be of the order of the spacing between fibers [Hlavacek (1975), (1976)], in cellular solids it may be comparable to the average cell size [Adomeit (1967); Berglund (1982)].

Consider a chiral Cosserat medium medium, in a Cartesian coordinates system (x,y,z). The equations of motion in the absence of body forces and body couples are [Eringen (1966), (1968); Mindlin (1964), (1965); Chiroiu, Munteanu and Gliozzi (2010)]

$$\sigma_{kl,k} - \rho \ddot{u}_l = 0, \quad m_{rk,r} + \varepsilon_{klr}\sigma_{lr} - \rho j \ddot{\varphi}_k = 0, \quad k,l = 1,2,3. \tag{3.1}$$

Here σ_{kl} is the stress tensor, m_{kl} is the couple stress tensor, u is the displacement vector, φ_k is the microrotation vector which in Cosserat elasticity is kinematically different from the macrorotation vector $r_k = \frac{1}{2}\varepsilon_{klm}u_{m,l}$, and ε_{klm} is the Levi-Civita

permutation symbol. We remember that φ_k refers to the rotation of points themselves, while r_k refers to the rotation associated with movement of nearby points. In (3.1) ρ is the mass density and j the microinertia. The constitutive equations are given by [Donescu, Chiroiu and Munteanu (2009)]

$$\sigma_{kl} = \lambda e_{rr}\delta_{kl} + (2\mu + \kappa)e_{kl} + \kappa\varepsilon_{klm}(r_m - \varphi_m) + C_1\varphi_{r,r}\delta_{kl} + C_2\varphi_{k,l} + C_3\varphi_{l,k},$$

$$m_{kl} = \alpha\varphi_{r,r}\delta_{kl} + \beta\varphi_{k,l} + \gamma\varphi_{l,k} + C_1 e_{rr}\delta_{kl} + (C_2 + C_3)e_{kl} + (C_3 - C_2)\varepsilon_{klm}(r_m - \varphi_m), \tag{3.2}$$

where $e_{kl} = (u_{k.l} + u_{l,k})/2$ is the macrostrain vector. λ, and μ are Lamé elastic constants, κ is the Cosserat rotation modulus and α, β, γ the Cosserat rotation gradient moduli, and C_i, $i = 1,2,3$, the chiral elastic constants associated with noncentrosymmetry [Cosserat (1909); Kröner (1963); Lakes and Benedict (1982); Lakes (2001)]. The materials which are not invariant to coordinates inversions can have a qualitatively different behavior in comparison with isotropic solids. An elastic chiral material (noncentrosymmetric material) is isotropic with respect to coordinate rotations but not with respect to inversions. For $C_i = 0$ the equations of isotropic micropolar elasticity are recovered. For$\alpha = \beta = \gamma = \kappa = 0$, (3.4) reduces to the constitutive equations of classical isotropic linear elasticity theory. From the requirement that the internal energy must be nonnegative (the material is stable), we obtain restrictions on the elastic constants $0 \leq 3\lambda + 2\mu + \kappa$, $0 \leq 2\mu + \kappa$, $0 \leq \kappa$, $-\gamma \leq \beta \leq \gamma$, $0 \leq \gamma$ and any positive or negative C_1, C_2, C_3 [Gauthier (1982); Lakes and Benedict (1982)].

By definition, the set composed of the asymmetric tensors σ_{kl}, m_{kl}, e_{kl}, $k,l = 1,2,3$, and the vectors u_k, φ_k, namely $\mathrm{F} = \{\sigma_{kl}, m_{kl},\ u_k, \varphi_k,\quad k,l = 1,2,3\}$ is said to be an elastodynamic state on the bounded medium, if it satisfies (3.1) and (3.2). It is easy to prove that the state F can be decomposited in the form

$$\mathrm{F} = \mathrm{F}_1 + \mathrm{F}_2, \tag{3.3}$$

where $\mathrm{F}_1 = \{\sigma_{11}, \sigma_{13}, \sigma_{33}, m_{22}, u_1, u_3, \varphi_2\}$ and $\mathrm{F}_2 = \{\sigma_{22}, m_{11}, m_{13}, m_{33}, u_2, \varphi_1, \varphi_3\}$ [Donescu, Chiroiu and Munteanu (2009)]. By introducing (3.2) into (3.1), after a proper manipulation of equations, the following equations in the unknowns $u = (u_1, u_2, u_3)$ and $\varphi = (\varphi_1, \varphi_2, \varphi_3)$ are found.

$$(\lambda + 2\mu + \kappa)\nabla\nabla u - (\mu + \kappa)K_0^2\nabla\times\nabla\times u + \kappa(1 - K_0^2)\nabla\times\varphi = \rho\ddot{u}, \tag{3.4}$$

$$(\alpha + \beta + \gamma)\nabla\nabla\varphi - \gamma K_0^2\nabla\times\nabla\times\varphi + \kappa(1 - K_0^2)\nabla\times u - 2\kappa(1 - K_0^2)\varphi = \rho j\ddot{\varphi}, \tag{3.5}$$

where

$$K_0^2 = 1 + \frac{(C_1 + C_2 + C_3)^2}{(\lambda + 2\mu + \kappa)(\alpha + \beta + \gamma)}.$$

We see that (3.4) and (3.5) are decoupled into two sets of equations with respect to F_1, F_2, respectively. For simplicity, without any loss of generality, the particular case in which all quantities depend only on x (radial direction r) and y (longitudinal direction) is considered. We will focus on the 2D set of equations corresponding toF_1, the other set being solved in a similar manner. By introducing the dimensionless quantities

$$x' = \frac{\omega}{c_1}x, \quad y' = \frac{\omega}{c_1}y, \quad v_i' = \frac{\omega}{c_1}u_i, \quad i = 1,2,$$

$$\phi_2' = \frac{\mu K_0^2}{\rho j \omega^2}\varphi_2, \quad t' = \omega t, \quad \sigma_{ij}' = \frac{1}{\mu K_0^2}\sigma_{ij},$$

$$m_{ij}' = \frac{c_1}{\gamma \omega K_0^2} m_{ij}, \quad \omega^2 = \frac{\kappa(1-K_0^2)}{\rho j}, \quad c_1^2 = \frac{\lambda + 2\mu + \kappa}{\rho}, \quad i,j = 1,3,$$

the equations (3.4) and (3.5) reduce to by suppressing the dashes

$$\begin{aligned}
&(s_1 + s_2)v_{1,xx} + s_1 v_{3,xy} + s_2 v_{1,yy} - s_3\phi_{2,y} + \omega^2 v_1 = 0,\\
&(s_1 + s_2)v_{3,yy} + s_1 v_{1,xy} + s_2 v_{3,xx} + s_3\phi_{2,x} + \omega^2 v_3 = 0,\\
&\phi_{2,xx} + \phi_{2,yy} - s_5\phi_2 + s_6(v_{1,y} - v_{3,x}) + s_4\omega^2\phi_2 = 0,
\end{aligned} \tag{3.6}$$

where

$$s_1 = \frac{\lambda + \mu K_0^2}{\rho c_1^2}, \quad s_2 = \frac{\kappa(1-K_0^2) + \mu K_0^2}{\rho c_1^2}, \quad s_3 = \frac{\kappa j(1-K_0^2)\omega^2}{\mu K_0^2 c_1^2},$$

$$s_4 = \frac{\rho j c_1^2}{\gamma k_0^2}, \quad s_5 = \frac{2c_1^2\kappa(1-K_0^2)}{\omega^2\gamma K_0^2}, \quad s_6 = \frac{c_1^2\mu}{\omega^2\gamma}. \tag{3.7}$$

The equations (3.6) can be rewritten under the form

$$\nabla \cdot S : \nabla U + \omega^2 U = 0, \tag{3.8}$$

where ρ is the scalar density of the elastic medium, S is the fourth-order material tensor, ω is the wave angular frequency, and $U(x_1,x_2,x_3,t) = U(x_1,x_2,x_3)\exp(-\mathrm{i}\omega t)$ is the vector defined as $U = (v_1, v_3, \phi_2)$. The equations (3.8) retain their form under this transforms (2.1), (2.3) and (2.5).

Under a change of coordinates (x',y',z') to (x,y,z) given by (3.1) such that $U'(x') = J^{-\mathrm{T}}_{x'x}U(x)$, J, eq. (3.8) takes the form

$$\nabla' \cdot S' : \nabla' U' + \omega'^2 U' = 0, \tag{3.9}$$

with $U' = (v'_1, v'_3, \phi'_2)$. Eqs. (3.9) can be written explicitly as

$$\begin{aligned}
&(s'_1 + s'_2)v'_{1,x'x'} + s'_1 v'_{3,x'y'} + s'_2 v_{1,y'y'} - s'_3 \phi'_{2,y'} + \omega'^2 v'_1 = 0,\\
&(s'_1 + s'_2)v'_{3,y'y'} + s'_1 v'_{1,x'y'} + s'_2 v'_{3,x'x'} + s'_3 \phi'_{2,x'} + \omega'^2 v'_3 = 0,\\
&\phi'_{2,x'x'} + \phi'_{2,y'y'} - s'_5 \phi'_2 + s'_6 (v'_{1,y'} - v'_{3,x'}) + s'_4 \omega'^2 \phi'_2 = 0,
\end{aligned} \tag{3.10}$$

with

$$\begin{aligned}
&s'_1 = \frac{\lambda' + \mu' K_0^2}{\rho' c'^2_1}, \quad s'_2 = \frac{\kappa'(1 - K'^2_0) + \mu' K'^2_0}{\rho' c'^2_1}, \quad s'_3 = \frac{\kappa' j (1 - K'^2_0)\omega'^2}{\mu' K'^2_0 c'^2_1}\\
&s'_4 = \frac{\gamma' K_0^2}{\rho' j c'^2_1}, \quad s'_5 = \frac{2c'^2_1 \kappa'(1 - K'^2_0)}{\omega'^2 \gamma' K'^2_0}, \quad s'_6 = \frac{c'^2_1 \mu'}{\omega'^2 \gamma'},\\
&K'^2_0 = 1 + \frac{(c'_1 + c'_2 + c'_3)^2}{(\lambda' + 2\mu' + \kappa')(\alpha' + \beta' + \gamma')},
\end{aligned} \tag{3.11}$$

where

$$\begin{aligned}
&\lambda' = \frac{\lambda}{\det(J_{xx'})}, \quad \mu' = \frac{\mu}{\det(J_{xx'})}, \quad \kappa' = \frac{\kappa}{\det(J_{xx'})},\\
&\alpha' = \frac{\alpha}{\det(J_{xx'})}, \quad \beta' = \frac{\beta}{\det(J_{xx'})}, \quad \gamma' = \frac{\gamma}{\det(J_{xx'})},\\
&\rho' = \frac{\rho}{\det(J_{xx'})}, \quad \kappa' = \frac{\kappa}{\det(J_{xx'})}, \quad \rho' = \frac{\rho}{\det(J_{xx'})}, \quad c'_i = \frac{C_i}{\det(J_{xx'})}, \quad i = 1,2,3.
\end{aligned} \tag{3.12}$$

When we change the coordinate system, automatically we replace the initial material properties by equivalent material properties given by (3.11) and (3.12).

4 Results

The original material is conventional closed-cell polyurethane foam with $\rho_{conv} = 27\text{kg/m}^3$ density and Poisson's ratio at tensile test $\nu_{tens} = 0.47$ and the compressive test $\nu_{comp} = 0.27$. The cylindrical specimen has $R_2 = 15\text{mm}$ initial radius and $l = 170\text{mm}$ initial length. The following constants are considered: $\lambda = 2.59\text{GPa}$, $\mu = 0.77\text{GPa}$, $\kappa = 0.0144\text{GPa}$, $\alpha = 1.77\times10^4\text{N}$, $\beta = 3.37\times10^4\text{N}$, $\gamma = 0.33\times10^4\text{N}$, $C_1 = -0.5\times10^4\text{N/m}$, $C_2 = -2.9\times10^4\text{N/m}$, $C_3 = -6.8\times10^4\text{N/m}$, $j = 2\times10^{-7}\text{m}^2$.

We must say that the condition of a positive Young's modulus and $-1 < \nu < 0.5$ corresponds to the usual range of properties for stability of the material. The existence of negative material constants (shear modulus, bulk modulus, stiffness) is also permitted (experimentally reported in Wang and Lakes (2004), Teodorescu *et al.* (2005a,b)).

The Poisson's ratio $\nu = \nu_{yx}$(for tensile and compressive tests) was calculated as the negative ratio between the radial and longitudinal strains using a best fit to the strain-strain graph

$$\nu_{yx} = -\frac{\varepsilon_x}{\varepsilon_y}. \tag{4.1}$$

The most important physical parameter to dominate the negative Poisson's ratio transformation is the compression ratio $\vartheta = \frac{(R'^2_2 - R'^2_1)l'}{R^2_2 l}$, where prime denotes the final parameters.

The existing methods concerning the solving of (3.10) are mainly based on the homogenization approach [Kumar and McDowell (2004)]. Another method is the missing ribs method by Smith *et al.* (2000). We solve the equations (3.12) by applying the Laplace and Fourier transforms.

Figure 4.1.shows the variation of the Poisoon's ratio with respect to $1-\vartheta$ (equivalent to the compressive strain) for conventional foam (the upper curve) and auxetic foam (the lower curve) respectively. We observe that the conventional foam becomes auxetic ($-0.15 < \nu < 0$) for$0.55 < 1-\vartheta < 0.77$, or $0.23 < \vartheta < 0.45$. It is very interesting to see that the auxetic foam is changing the sign for its Poisson's ratio for$0.46 > 1-\vartheta$. It is of interest to underline that the results provides an overall agreement with the experimental values for the auxetic foam [Bezazi and Scarpa (2007); Shilko and Konyok (2004)].

The initial domain with $R_2 = 15\text{mm}$ and $l = 170\text{mm}$ is transformed into a shell cylinder with $l' = 100\text{mm}$, $R'_2 = 15\text{mm}$ and $14.415\text{mm} < R'_1 < 14.7\text{mm}$. The transformed annulus domains are presented in Fig. 4.2, for $\vartheta = 0.25$, 0.26, 0.3 and 0.4.

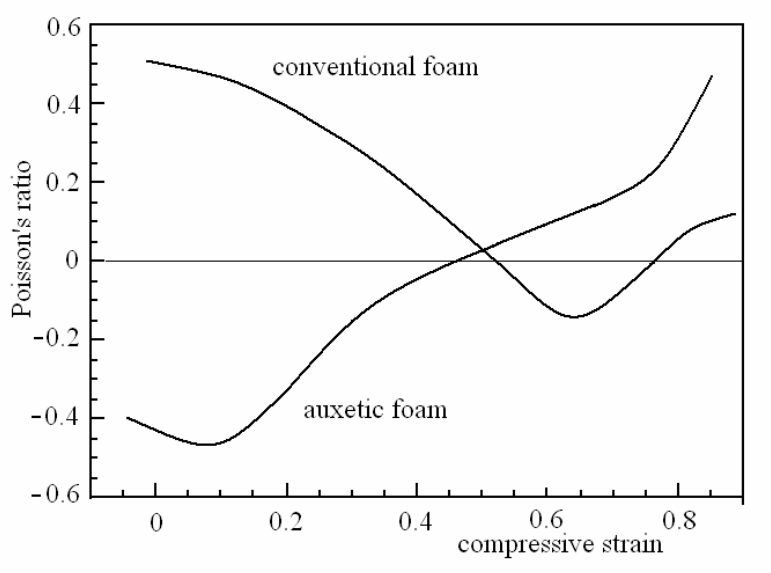

Figure 4.1: Poisson's ratio versus compressive strain for conventional and auxetic foams.

Let us introduce three reduced moduli defined as

$$K'_1 = \frac{K'^2_{10}}{K^2_0}, \quad K'_2 = \frac{K'^2_{11}}{K'^2_0}, \quad K'_3 = \frac{K'^2_{12}}{K'^2_0}, \tag{4.2}$$

where K^2_{10}, K^2_{11} and K^2_{12} are given by

$$K^2_{10} = \frac{(c'_2 + c'_3)^2}{4(2\mu' + \kappa')(\beta' + \gamma')}, \quad K^2_{11} = \frac{(c'_2 - c'_3)^2}{4(2\mu' + \kappa')(\gamma' - \beta')}, \tag{4.3}$$

$$K^2_{12} = \frac{(3c'_1 + c'_2 + c'_3)^2}{4(3\lambda' + 2\mu' + \kappa')(3\alpha' + \beta' + \gamma')},$$

and K'^2_0 is given by $(3.11)_3$.

The dependence of the properties of the auxetic foam on the Poisson's ratio ν and the coordinates is illustrates next. The variation of the reduced moduli on ν is displayed in Figure 4.3. For a given ν it is possible to determine a set of permissible material constants, negative or not.

Each set of constants may represent a certain possible structure with demonstrable auxetic properties. The variation of the Young's modulus with respect to radial

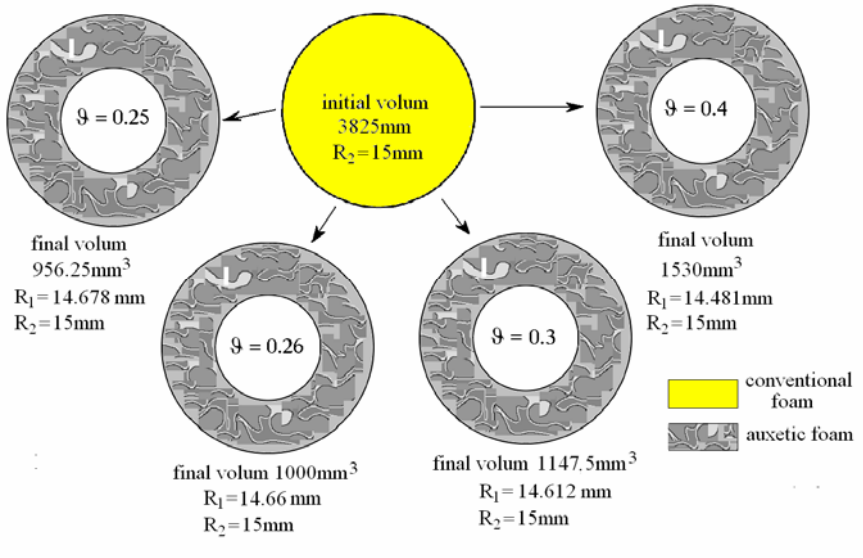

Figure 4.2: Transformed domains.

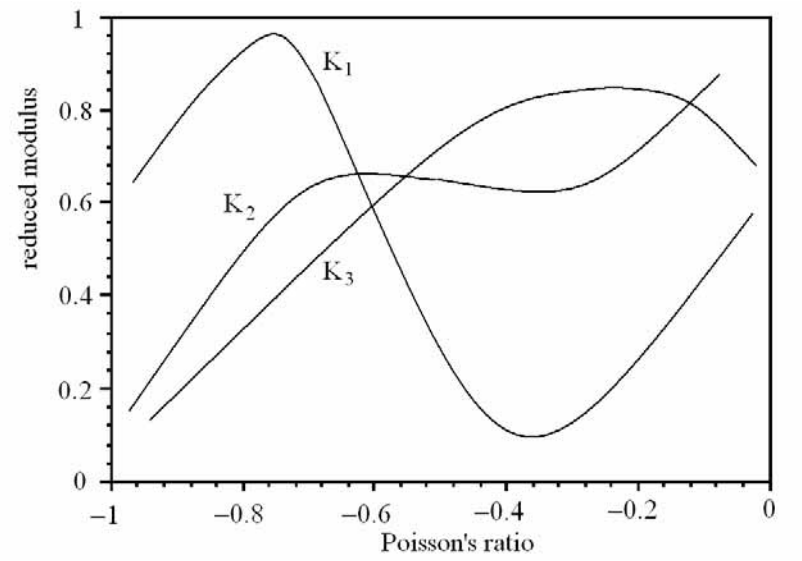

Figure 4.3: Reduced moduli versus Poisson's ratio.

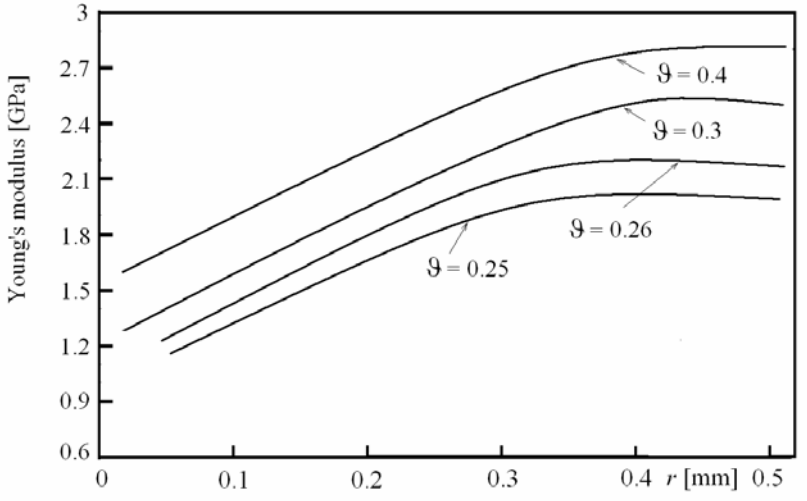

Figure 4.4: Variation of the Young's modulus with respect to radial coordinate.

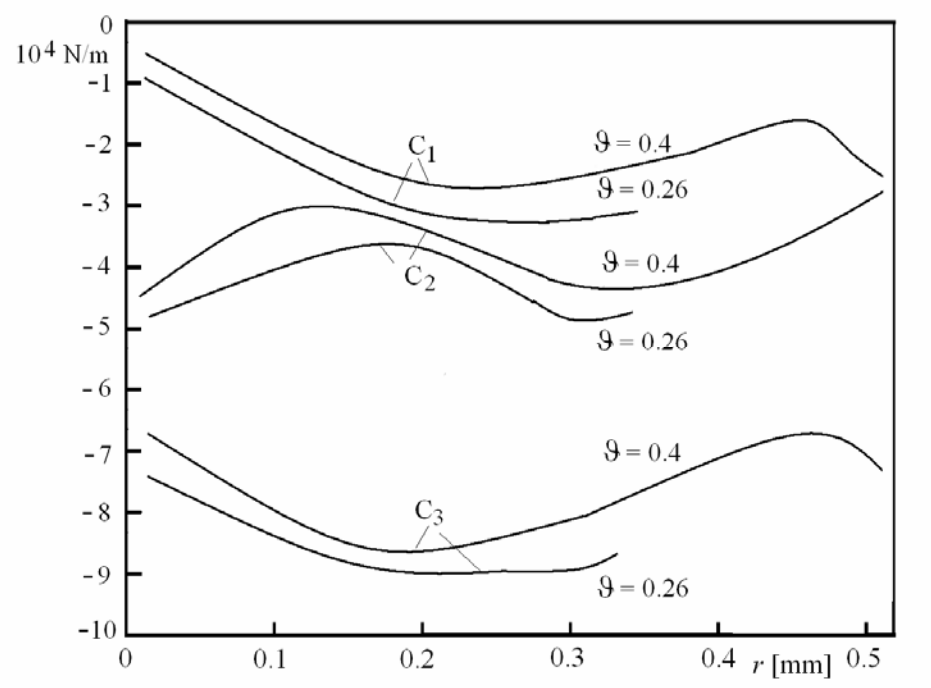

Figure 4.5: Variation of the chiral elastic constants$C_1, C_2, C_3$with respect to radial coordinate.

coordinate $R_1 \leq r \leq R_2$ is presented in Figure 4.4 for ϑ =0.25, 0.26, 0.3 and 0.4 (the corresponding thicknesses for the annulus $R_1 \leq r \leq R_2$ are 0.322mm, 0.34mm, 0.3888 and 0.519 respectively).

The variation of the chiral elastic constantsC_1, C_2 and C_3 with respect to radial coordinate r is illustrated in Figure 4.5, for ϑ =0.26 and 0.4. We see that these constants are negative.

5 Conclusions

A new technique for transforming the conventional foams into auxetic foams is proposed in this paper by exploiting the property of the governing equations to be written in a covariant form such that the metric is only involved in the material parameters. The geometric transformations lead to material properties that are, if not impossible to obtain, at least challenging for manufacture of new materials.

Acknowledgement: This research was elaborated through the PN-II-PT-PCCA-2011-3.1-0190 Project of the National Authority for Scientific Research (ANCS, UEFISCSU), Romania. The authors acknowledge the similar and equal contributions to this article.

References

Adomeit, G. (1967): Determination of elastic constants of a structured material, *Mechanics of Generalized Continua* (Edited by Kröner, E.), IUTAM Symposium, Freudenstadt, Stuttgart. Springer, Berlin.

Akbarov, S.D.; Kosker, R.; Ucan, Y. (2010): A novel framework for building materials knowledge systems. *CMC: Computers, Materials & Continua* 17(2): 103–126.

Alderson K.L.; Alderson A.; Evans K.E. (1997): The interpretation of strain dependent Poisson's ratio in auxetic polyethylene. *J. Strain Anal*. 32: 201–212.

Alu, A.; Engheta, N. (2003): Pairing an epsilon-negative slab with a miu-negative slab: resonance, tunneling and transparency, *IEEE Trans. Antennas Propag*. 51: 2558–2571.

Alu, A., Engheta, N. (2005): Achieving transparency with plasmonic and metamaterial coatings, *Phys. Rev. E* 72: 016623.

Blake, A.; Isard, M. (1998): Active contours – the application of techniques from graphics, vision, control theory and statistics to visual tracking of shapes in motion. *London: Springer*.

Berglund, K. (1982): Structural models of micropolar media, in *Mechanics of*

Micropolar Media, edited by O. Brulin and R. K. T. Hsieh, World Scientific, Singapore.

Bezazi, A.; Scarpa, F. (2007): Mechanical behaviour of conventional and negative Poisson's ratio thermoplastic polyurethane foams under compressive cyclic loading. *International Journal of Fatique* 29: 922–930.

Bigoni, D.; Serkov, S.K.; Valentini, M.; Movchan, A.B. (1998): *Int. J. Solids Structures*. 35: 3239.

Brun, M. ; Guenneau, S. ; Movchan, A.B. (2009) : Achieving control of in-plane elastic waves. *Applied Physics Letters* 94: 061903.

Chan, N.; Evans, K.E. (1997): Fabrication methods for auxetic foams. *J. Mat. Sci*. 32: 5725–5736.

Chekkal, I.; Bianchi, M.; Remillat, C.; Bécot, F.X.; Jaouen, L.; Scarpa, F. (2010): Vibro-acoustic properties of auxetic open cell foam:model and experimental results. *Acta Acustica United with Acustica* 96: 266–274.

Chen, C.P.; Lakes. R.S. (1989): Dynamic wave dispersion and loss properties of conventional and negative Poisson's ratio polymeric cellular materials. *Cellular Polymers* 8: 343–369.

CHIROIU, V.; MUNTEANU, L.; DUMITRIU, D.; BELDIMAN, M.; SECARA, C. (2008): ON THE ARCHITECTURE OF A NEW CELLULAR ELASTIC MATERIAL. *PROCEEDINGS OF THE ROMANIAN ACADEMY, SERIES A: MATHEMATICS, PHYSICS, TECHNICAL SCIENCES, INFORMATION SCIENCE* 9(2): 105–115.

Chiroiu, V.; Munteanu, L.; Gliozzi, A.S. (2010): Application of Cosserat theory to the modeling of reinforced carbon nanotube beams. *CMC: Computers, Materials & Continua*. 19(1): 1–16.

Cosserat, E. and F. (1909): Théorie des Corps Deformables, *Hermann et Fils*, Paris.

Cummer, S.A. ; Popa, B.I. ; Schurig, D. ; Smith, D.R. ; Pendry, J. ; Rahm, M. ; Starr, A. (2008): Scattering theory derivation of a 3D acoustic cloaking shell. *Physical Review Letters* 100: 024301.

Cummer, S.A.; Schurig, D. (2007): One path to acoustic cloaking. *New Journal of Physics* 9: 45–52.

Donescu, ?t.; Chiroiu, V.; Munteanu, L. (2009): On the Young's modulus of an auxetic composite structure. *Mechanics Research Communications* 36(3): 294–301.

Donescu, St.; Munteanu, L.; Delsanto, P.P.; Mosnegutu, V. (2009): On the advanced auxetic composites. *Research Trends in Mechanics*, Publishing House of

the Romanian Academy 3: 78–93.

Dupont, G.; Farhat, M.; Diatta, A.; Guenneau, S.; Enoch, S. (2011): Numerical analysis of three-dimensional acoustic cloaks and carpets. doi: abs/1103.1081.

Eringen, A.C. (1966): Linear theory of micropolar elasticity. *J. Math. & Mech*. 15: 909–924,

Eringen, A.C. (1968): Theory of micropolar elasticity, *Fracture* (ed. R. Liebowitz), 2, Academic Press, 621–729.

Evans K.E. (1991): Auxetic polymers: a new range of materials. *Endeavour New Ser.* 15: 170–174.

Evans, K.E.; Alderson, A. (2000): Auxetic materials: Functional materials and structures from lateral thinking. *Advanced materials* 12(9): 617–628.

Fu, Z-J.; Chen,W.; Qin, Q-H. (2011): Hybrid finite element method based on novel general solutions for Helmholtz-type problems. *CMC: Computers, Materials & Continua* 21(3): 187–208.

Gauthier, R.D. (1982): Experimental investigations on micropolar media, 395–463, in: Mechanics of Micropolar Media. *CISM Courses and lectures*, edited by O. Brulin and R.K.T. Hsieh, World scientific.

Gaspar, N.; Ren, X.J.; Grima, J.N.; Smith, C.W.; Evans, K.E. (2005): Novel honeycombs with Auxetic behaviour. *Acta Materialia* 53: 2439–2445.

Greenleaf, A.; Lassas, M.; Uhlmann, G. (2003): On nonuniqueness for Calderons inverse problem. *Math. Res. Lett*. 10: 685–693.

Guenneau, S.; McPhedran, R.C.; Enoch, S.; Movchan, A.B.; Farhat, M.; Nicorovici, N.A. (2011): The colours of cloaks. *Journal of Optics* 13(2): 024014.

Hlavacek, M. (1975): A continuum theory for fibre reinforced composites, *Int. J. Solids and Structures* 11: 199–211.

Hlavacek, M. (1976): On the effective moduli of elastic composite materials. *Int. J. Solids and Structures* 12: 655–670.

Johansson, B.T.; Marin, L. (2009): Relaxation of alternating iterative algorithms for the Cauchy problem associated with the modified Helmholtz equation. *CMC: Computers, Materials & Continua* 13(2): 153–190.

Kalidindi, S.R.; Niezgoda, S.R.; Landi, G.; Vachhani, S.; Fast, T. (2010): A novel framework for building materials knowledge systems. *CMC: Computers, Materials & Continua* 17(2): 103–126.

Kröner, E. (1963): On the physical reality of torque stresses in continuum mechanics. *Int. J. Engng. Sci.*, 1: 261–278.

Kumar, R.S.; McDowell, D.L. (2004): Generalized continuum modeling of 2-D

periodic cellular solids. *Int. Journal of Solids and Structures* 4: 7399–7422.

Lakes, R.S. (1986): Experimental Microelasticity of Two Porous Solids. *Int. J. Solids Structures* 22: 55–63.

Lakes, R.S. (1987): Foam structures with a negative Poisson's ratio. *Science* 235: 1038–1040.

Lakes, R.S. (1991): Experimental micro mechanics methods for conventional and negative Poisson's ratio cellular solids as Cosserat continua. *J. Engineering Materials and Technology* 113: 148–155.

Lakes, R.; Elms, K.J. (1993): Indentability of conventional and negative Poisson's ratio foams. *Comp Math*. 27: 1193–1202.

Lakes, R.S.; Benedict, R.L. (1982): Noncentrosymmetry in micropolar elasticity. *Int. J. Engng. Sci.* 20(10): 1161–1167.

Lakes, R.S. (2001): Elastic and viscoelastic behaviour of chiral materials. *Int. J. of Mechanical Sciences* 43: 1579–1589.

Leonhardt, U. (2006): Optical conformal mapping. *Science* 312: 1777–1780.

Marin, L.; Karageorghis, A. (2009): Regularized MFS based boundary identification in two dimensional Helmholtz type equations. *CMC: Computers, Materials & Continua* 10(3): 259–294.

Mihailescu, M.; Chiroiu, V. (2005): Advanced mechanics on shells and intelligent structures. *Publishing House of the Romanian Academy,* Bucharest.

Milton, G.W.; Briane, M.; Willis, J.R. (2006): On cloaking for elasticity and physical equations with a transformation invariant form. *New Journal of Physics* 8: 248.

Milton, G.W.; Nicorovici, N.A. (2006): On the cloaking effects associated with anomalous localized resonance. *Proc. Roy. Soc.* A 462: 3027–3059.

Milton, G.W. (2007): New metamaterials with macroscopic behavior outside that of continuum elastodynamics. *New Journal of Physics* 9: 359– 372.

Mindlin, R.D. (1964): Microstructure in linear elasticity. *Arch. Rat. Mech. Anal*. 16: 51–78.

Mindlin, R.D. (1965): Stress functions for a Cosserat continuum. *Int J. Solids Structures* 1: 265–271.

Munteanu, L.; Chiroiu, V. (2011): On the three-dimensional spherical acoustic cloaking. *New Journal of Physics* 13(8): 083031.

Munteanu, L.; Dumitriu, D.; Donescu, St.; Chiroiu, V. (2009): On the complexity of the auxetic systems. *Proc.of the European Computing Conference*, Lecture Notes in Electrical Engineering, 28(2): 1543–1549.

Munteanu, L.; Donescu, St.; Delsanto, P.P.; Dumitriu, D.; Mosnegutu, V. (2008): On the characterization of auxetic materials. *Research Trends in Mechanics* vol.2, Publishing House of the Romanian Academy (eds. D.Popa, V.Chiroiu, I.Toma).

Norris, A. (2008): Acoustic cloaking theory. *Proc. Roy. Soc*. A 464: 2411–2434.

Pendry, J.B.L; Shurig, D.; Smith, D.R. (2006): Controlling electromagnetic fields. *Science* 312: 1780–1782.

Scarpa, F.; Pastorino, P.; Garelli, A.; Patsias, S.; Ruzzene, M. (2004): Auxetic compliant flexible PU foams: static and dynamic properties. *Phys Stat Solid B* 242(3): 681–694.

Scarpa, F.; Ciffo, L.G.; Yates, J.R. (2004): Dynamic properties of high structural integrity auxetic open cell foam. *Smart Mater Struct*. 13: 49–56.

Shilko, S.; Konyok, D. (2004): Numerical and experimental study of auxetic closed-cell foams. *Computational methods in Science and Technology* 10(2): 197–202.

Smith, C.W.; Grima, J.N.; Evans, K.E. (2000): A novel mechanism for generating auxetic behaviour in reticulated foams: missing rib foam model. *Acta Materialia* 48: 4349–4356

Teodorescu, P.P.; Munteanu, L.; Chiroiu, V. (2005a): On the wave propagation in chiral media, New Trends in Continuum Mechanics. *Theta Series in Advanced Mathematics* (ed. M.Mihailescu-Suliciu), Editura Thetha Foundation, Bucharest, 303–310.

Teodorescu, P.P.; Badea, T.; Munteanu, L.; Onisoru, J. (2005b): On the wave propagation in composite materials with a negative stiffness phase, New Trends in Continuum Mechanics. *Theta Series in Advanced Mathematics* (ed. M.Mihailescu-Suliciu), Editura Thetha Foundation, Bucharest, 295–302.

Zolla, F.; Guenneau, S.; Nicolet, A.; Pendry, J.B. (2007) : Electromagnetic analysis of cylindrical invisibility cloaks and the mirage effect. *Opt. Letters* 32: 1069–1071.

Wang, Y-C.; Lakes, R. (2004): Negative stiffness-induced extreme viscoelastic mechanical properties:stability and dynamics. *Philosophical Magazine* 84(35): 3785–3801.

Wang, Y.C.; Lakes, R.S.; Butenhoff, A. (2001): Influence of cell size on re-entrant transformation of negative Poisson's ratio reticulated polyurethane foams. *Cellular Polymers* 20: 373–385.